PCCP

Nanopore Facilitated Monohydrocalcitic Amorphous Calcium Carbonate Precipitation

Journal:	*Physical Chemistry Chemical Physics*
Manuscript ID	CP-ART-01-2022-000446.R1
Article Type:	Paper
Date Submitted by the Author:	17-Jun-2022

Complete List of Authors:	Page, Katharine; University of Tennessee Knoxville College of Engineering, Materials Science and Engineering Department; Oak Ridge National Laboratory, Neutron Scattering Division Stack, Andrew; Oak Ridge National Laboratory, Chemical Sciences Division Chen, Si Athena; Oak Ridge National Laboratory, Chemical Sciences Division Wang, Hsiu-Wen; Oak Ridge National Laboratory, Chemical Sciences Division

ARTICLE

Nanopore Facilitated Monohydrocalcitic Amorphous Calcium Carbonate Precipitation

Received 00th January 20xx,
Accepted 00th January 20xx

DOI: 10.1039/x0xx00000x

Katharine Page,*[a,b] Andrew G. Stack,[c] Si Athena Chen[c] and Hsiu-Wen Wang*[c]

Predicting the precipitation of solids is important in both natural systems and subsurface energy applications. The factors controlling reaction mechanisms, phase selection and conversion between phases are particularly important. In this contribution the precipitation and growth of an amorphous calcium carbonate species from flowing aqueous solution in a nanoporous controlled pore glass is followed *in situ* with differential X-ray pair distribution function analysis. It is discovered that the local atomic structure of this phase indicates monohydrocalcite-like pair-pair correlations, yet is functionally amorphous because it lacks long-range structure. The unexpected occurrence of synthetic proto-monohydrocalcite amorphous calcium carbonate, precipitated from a solution undersaturated with respect to published solubilities, suggests that nanopore confinement facilitates formation of an amorphous phase at the expense of more favorable crystalline ones. This result illustrates that confinement and interface effects are physical factors exerting control on mineral nucleation behavior in natural and geological systems.

Introduction

There are five crystalline calcium carbonate minerals: the three anhydrous phases, calcite, aragonite, and vaterite; and the two hydrous phases, monohydrocalcite and ikaite. Some of these phases are ubiquitous in the subsurface and play a central role in energy-relevant applications such as scale formation during oil and gas production, carbon sequestration, and transport of toxic metal contaminants. Amorphous calcium carbonate, ACC ($CaCO_3 \cdot nH_2O$) is significant in biomineral formation, and is recognized as one of the possible precursors in the formation of crystalline carbonate minerals based on the high energy barrier for homogeneous calcite nucleation in accordance with classical nucleation theory[1-4] (e.g., approximately 169 kJ/mol energy barrier[4] for formation of ~0.8 nm critical radii using saturation index of 2 and interfacial energy of 117 mJ/m^2). At the same time, there is significant evidence that biogenic ACC exists in a variety of polyamorphic forms; that is, various forms exhibit short-range order matching local atomic bonding of specific crystalline polymorphs.[2,5,6] It has been shown that synthetic forms of ACC can be made: aragonitic-ACC by applied pressure,[7] proto-calcite and proto-vaterite by slow-dosing fixed pH method,[2,8] monohydrocalcitic-amorphous (basic) calcium carbonate (A(B)CC) by fast centrifugal mixing,[9] and ACC without a clear crystalline analog.[10] It has also been shown that a rich amorphous polytypism and stabilization mechanism exist in additive stabilized ACCs.[11-18] It has been suggested that these various "pre-structured" forms could determine crystallization pathways,[2,11,19] yet some results point to the contrary.[15,16,20,21] For example, it is argued that ACC crystallization is not controlled by its structural motifs, because ACCs synthesized under various conditions all show similar short- and medium-range order.[16,20] Instead, the transformation pathways are kinetically governed by ion impurities (e.g., Mg^{2+}, PO_4^{3-}, OH^-) and water content.[15,16,20,21] Although the presence of specific protocrystalline structural motifs is still under debate, more recent results utilizing synthesis of pure compounds point to the effect of pH and cooperation of hydroxide ions (in addition to water molecules) as the key factors in stabilizing and controlling atomic scale changes in A(B)CC structure.[8,20] The use of (m)ethanol is also known to assist in stabilizing ACC nanoparticles precipitated directly from homogeneous calcium carbonate solution.[22-24] Mineral precipitation within localized environments is fundamental to biomineralization and subsurface heterogeneous nucleation processes, providing an alternative mechanism for stabilizing amorphous precursors. For example, it has been demonstrated that lipid vesicles can extend the lifetime of ACC before crystallization,[25] and confinement alone provides an effective inorganic mimic of the spicule environment that stabilizes ACC.[26,27] The presence of porous media (a certainty in the subsurface) is a key factor that will affect precipitation reactions, and on that subject much contradictory evidence has arisen, including concepts for heterogeneous precipitation across all surface area regardless of pore size, for nucleation suppression in small pores, and precipitation enhancement in small pores.[3] Stack et al.[28]

[a] *Materials Science and Engineering Department, The University of Tennessee, Knoxville, TN 38996, USA.*
[b] *Neutron Scattering Division, Oak Ridge National Laboratory, Oak Ridge, TN 37831, USA.*
[c] *Chemical Sciences Division, Oak Ridge National Laboratory, Oak Ridge, TN 37831, USA.*
** K.P.: kpage10@utk.edu, H.-W.W.: wanghswen@gmail.com*

Electronic Supplementary Information (ESI) available: Details of experiment procedures and crystalline reference material datasets, refinements, and models. See DOI: 10.1039/x0xx00000x

previously demonstrated via in-situ small angle X-ray scattering (SAXS) that growth of $CaCO_3$ in nanoporous silica matrix displays surface chemistry and pore-size dependent effects. Key uncertainties in debates over crystallization are the structure of initial nuclei, and how those structures develop during crystal growth. Thus, here we explore the nature of calcium carbonate precipitation and growth in confined nanopores with in-situ X-ray pair distribution function (PDF) measurements, increasingly used for structural studies of adsorbed, absorbed, or precipitated species on the surfaces of porous and nanocrystalline materials.[e.g.,29-33] Our results reveal the formation of a monohydrocalcite-like amorphous calcium carbonate from a moderate pH (8.4) solution that is undersaturated with respect to monohydrocalcite, ikaite, and ACC phases (Table 1). Its occurrence inside pores demonstrates alternative mechanisms (alternative to ion impurity incorporation) of stabilization and control over the structure of initial nuclei. This observation has direct implications on the importance of confinement in the thermodynamic and kinetic control of mineral nucleation in geological fluid-pore environments.

Experimental

In-situ X-ray PDF measurements were completed at the 11-ID-B instrument,[34] at The Advanced Photon Source at Argonne National Laboratory, utilizing a beam size of 500 µm by 500 µm, a photon energy of 58.65 keV (λ = 0.2114 Å), and a Perkin Elmer amorphous silicon image plate detector. A controlled-pore glass with nominal nanopore diameter of 24 nm (CPG-240, Millipore, Lincoln Park, NJ, USA), was loaded in a 1.6 mm polyaniline capillary fitted with a frit and ferrule with a 2 µm sieve, encased with a compression ring, and connected to a peristaltic pump (Masterflex model no. 7520-50) through Tygon tubing. The assembly was mounted vertically in the X-ray beam and aligned. The experimental setup is shown in Figure S1. A 1 L growth solution with a constant supersaturation of calcium carbonate was prepared immediately prior to the start of the experiment by mixing 964.5 mL of DI water (18.2 mΩ-cm) with 18.5 mL of 0.1M $CaCl_2$ (Sigma-Aldrich, 223506, Reagent, ≥99%) and 17.0 mL of 0.1M $NaHCO_3$ (Sigma-Aldrich, S6014, Reagent, ≥99.7%) stock solutions. All stock solutions were equilibrated with the atmosphere CO_2(g) for a week, ensuring the reported pH of the growth solution does not change over the course of the experiment. The composition of the growth solution was determined to have a $[Ca^{2+}]/[CO_3^{2-}]$ ratio of 90±1 and pH of 8.40±0.01 at 25 °C, estimated using the PHREEQC code with the LLNL database.[35] The saturation index (SI) of this solution relative to the known carbonate phases is provided in Table 1.

We note here that the SI of ~0.75 (with respect to calcite, Table 1) and calcium-to-carbonate ratio of ~90:1 present a condition close to the maximum calcite growth rate based on the growth model shown by Stack[36] (and references therein). In addition, the composition of the growth solution is also similar to solutions used in our previous SAXS works, where growth of $CaCO_3$ in nanoporous silica matrix displays surface chemistry effects.[28] The solutions are apparently metastable, with no visible homogeneous precipitation in the solution reservoir.

Solution was flowed through the CPG-filled column at a flow rate of 100 mL/h. Data was collected in 10-minute intervals starting from the time the fluid front passed through the cell. Data for samples of crystalline calcite, aragonite, and monohydrocalcite, as well as neat synthetic A(B)CC were collected for reference. The calcite and aragonite samples are natural specimens from the personal collection of H.-W.W. The monohydrocalcite is from the Department of Mineral Sciences, Smithsonian Institution (NMNH 1354040 00). The measured X-ray PDFs of calcite, aragonite and monohydrocalcite shown in Figure S2 are published in Wang et al.[9] Further details of the experimental setup are provided in the Supplementary Information.

Table 1. Saturation Index (SI) of the $CaCO_3$ growth solution used in this study with respect to known carbonate phases. SI = $\log(a_{Ca}a_{CO3}/K_{sp})$, and K_{sp} = solubility product.

Phase	$-\log(K_{sp})$ at 25 °C	SI
Calcite	8.48(2)[37,38]	0.75(2)
Aragonite	8.34(2)[37,38]	0.60(2)
Vaterite	7.91(2)[38]	0.17(2)
Monohydrocalcite	7.15(10)[39]	-0.6(1)
Ikaite	7.46(1)[39], 6.58(2)[40]	-0.28(1), 1.16(2)
ACC	6.39(2)[39,41], 6.0(3)[42]	-1.35(2), -1.7(3)
ACC I & II	~ 7.51[2] & 7.422[2]	~ -0.23 & -0.32

Results and discussion

Time-resolved X-ray PDFs, G(r), of a carbonate solution flowing through a CPG substrate are shown in Figure 1, where the normalized difference PDF ΔG(r) in Figure 1(a) is produced by correcting the ΔG(r) in Figure 1(b). The as-collected data in Figure 1(c) is dominated by the structural correlations of the CPG framework, which is amorphous SiO_2. Difference PDFs in Figure 1(b), ΔG(r), created by subtracting the first 10 minutes of collected data from each dataset, exhibit both negative (corresponding to shifting amounts of CPG in the X-ray beam) and positive (corresponding to carbonate species) pair-pair correlations growing with time. Thus, the amount of subtracted SiO_2 background is adjusted by removing negative correlations (arrows pointing down) coinciding with the SiO_2 framework structure, and is removed from the final data by applying a background scale factor that minimizes intensity at the Si-O pair-pair correlation at ~1.64 Å. The first few correlations match known carbonate, calcium, and water-oxygen pair-pair distances (e.g., intramolecular C-O_c at ~1.3 Å and O_c-O_c at ~2.4 Å, and intermolecular Ca-O_c/O_w at ~2.4 Å; see Wang et al.[9]). The observed structure is amorphous: there are no structural correlations at distances larger than 8 Å in real space. This agrees well with the absence of lattice fringes observed with transmission electron microscopy (TEM) for carbonate solution flow precipitates in CPG.[28]

Figure 2(a) shows the final 300 minute data set for the precipitated phase compared with data collected for neat A(B)CC, which we have reported[9] to qualitatively match ACC X-

ray PDF data reported by e.g., Tobler et al.[20], Michel et al.[43] and

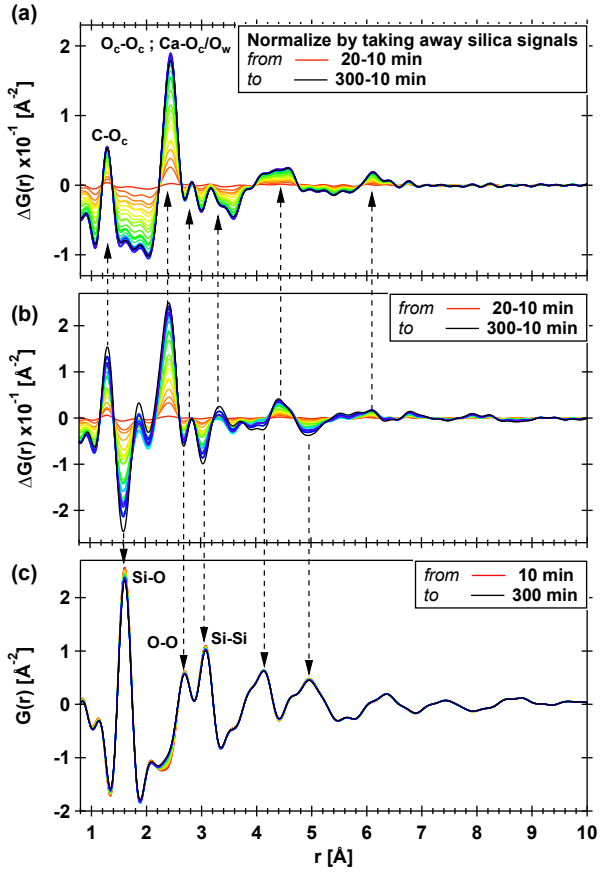

Figure 1. (a) Normalized difference PDFs every 10 minutes relative to the first dataset, corrected for diminishing signal from the CPG substrate. (b) Raw difference PDFs. (c) Total time resolved experimental X-ray PDFs as a function of time. In all panels the first data set (completed at 10 minutes after the start of flow) is shown in red, and the final data set (collected between 290 and 300 minutes) is shown in black. Data in both (a) and (b) are shown at 10 times scale relative to (c). Arrows indicate relationships between datasets.

modeled by Goodwin et al.[44] These X-ray PDF data, including ours,[9] have been recently re-examined and carefully modelled by ab initio molecular dynamics simulations,[45] which show disordered structural correlation and the local Ca coordination environment in these neat A(B)CCs does not indicate strong relation to any crystalline analog. While the precipitated data share some gross features with the previously-measured neat A(B)CC, the intensity and width of the first (C-O_c) correlation are poorly matched, and position and intensities of correlations between 3.5 Å and 5.5 Å vary significantly (attributed to groups of Ca-Ca and Ca-O_c/O_w correlations, respectively). Is the precipitated ACC an amorphous polytype of a particular crystalline phase instead? Figure 2(b) shows refinement results for the local atomic structure of the collected amorphous precipitate data using the crystalline polymorph models shown in Figure S2. All models match the approximate location and shape of the C-O_c correlation at 1.3 Å and the Ca-O_c/O_c-O_c correlations at 2.4 Å. However, the match to the data for the bulk monohydrocalcite model agrees remarkably well with the precipitate structure across the complete range, and is also a significant improvement relative to agreement with neat A(B)CC data displayed in Figure 2(a). The scattering length density fitted in the previous SAXS analysis[28] was found to be close to that of monohydrocalcite, rather than calcite, and was attributed to a simplistic model in the original work. Since our local structure observations corroborate well with the previous TEM observations and SAXS modelling for a similar experimental setup, we conclude that the precipitating phase can be described as monohydrocalcitic-ACC.

The SI of the growth solution (Table 1) indicates that thermodynamically favorable growth conditions are present for calcite, aragonite, or vaterite, but not monohydrocalcite, ikiate or ACCs. Monohydocalcite is well known to be metastable with respect to calcite and vaterite,[46] though it has been observed in air conditioning systems,[47] in moonmilk deposits in caves (water/spray environments),[48] in biological systems,[49-51] and can be formed via Mg-rich ACC precursors.[11,52] The presence of Mg in solution is known to inhibit the formation of vaterite and calcite, preferring direct incorporation into monohydrocalcite.[53] The formation of monohydrocalcitic-ACC under flowing conditions in nanopores, from a solution that is Mg-free, is therefore a surprising result. It suggests that the confined fluid in nanopores creates an environment favorable for amorphous phases to form at lower supersaturations than for other pathways. For comparison, we also conducted a control flow through experiment where CPG substrate was replaced by silica glass microbeads (90-150 μm diameter) to create micron-sized porous environments (see Supplementary Information for details). We observed that calcite crystals readily grow on the surface of the glass microbeads, using the same growth solution composition as is used in the CPG experiment. This finding contrasts from the observed monohydrocalcitic-ACC precipitation/growth in nanopore environments and confirms that the nanoporous silica matrix pore size alters $CaCO_3$ heterogeneous growth behavior. Heterogeneous nucleation and growth of minerals from undersaturated conditions have

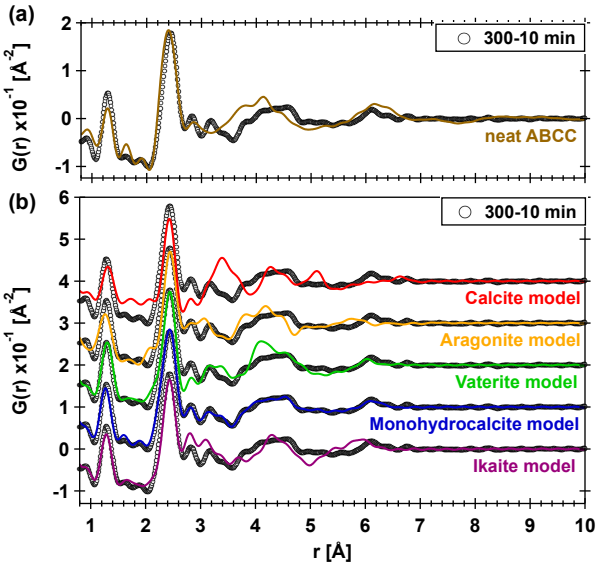

Figure 2. (a) A comparison of the precipitated phase data at 300 minutes (open grey circles) to an amorphous basic calcium carbonate data set (mustard line). (b) Comparison of the data with structure refinement results based on models from Figure S2.

Figure 3. (a) The refined correlation length scale (as *spdiameter*[57]) and final R_w values from each fit. (b) The refined scale factor (in black) of the monohydrocalcite structural model from each data set, along with the scale factor applied to remove silica signal (in blue) from the final ΔG(r). The measured concentration of Si in solution is shown in yellow in ppm.

been reported by Deng et al.,[54] utilizing a different system setup and implicating distinct mechanisms. In their work, heterogeneous nucleation of Sr-rich $(Ba_x,Sr_{1-x})SO_4$ from undersaturated bulk solution, and the formation of barites with Sr-levels that are thermodynamically unfavorable were observed on glass slides coated with a self-assembled monolayer. Organic films are found to enrich cation concentrations from bulk solution, increase the local supersaturation, and promote formation of Sr-rich barite nuclei.[54] The experiments here suggest the confinement effects may be playing a similar role by modifying the local environment in which the precipitation occurs.

The time-evolution of the difference PDF signals enables further examination of the nature of monohydrocalcitic-ACC precipitation in CPG. Figure 3 displays the time dependence of refinement model parameters and goodness of fit, R_w, for the series, along with the scale factor needed to remove changing silica intensities (see Supplementary Information). The nearly constant correlation length scale and the minimal changes in R_w indicate a consistent amorphous monohydrocalcitic motif with time (Fig. 3(a)). The amount of precipitated material (as reflected by the refined scale factor) indicates nearly linear accumulation over the first 150 minutes, slowing beyond approximately 200 minutes (Fig. 3(b)). The observed cessation of growth, along with the earlier SAXS results showing that ACC never completely fills available pores,[28] suggests the precipitate reaches a steady state in silica nanopores, perhaps as an interfacial thin layer. If this amorphous monohydrocalcitic-ACC were a viable precursor for calcite in this environment, it might

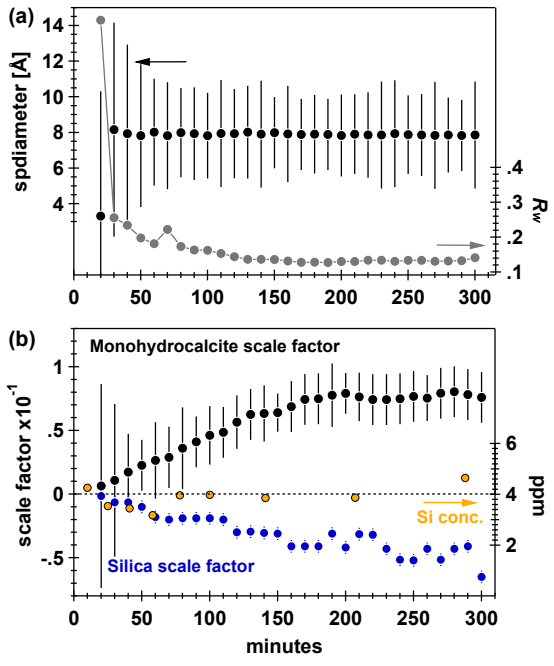

be expected to convert to calcite but such growth behaviors are not observed over the limited time-scales in this experiment or in previous work.[28]

This surprising result may be qualitatively rationalized using classical nucleation theory applied to heterogeneous nucleation, in which the overall thermodynamic stability of a nucleus is expressed in terms of bulk and surface free energies.[4,55] The latter is a function of three component interfacial energies: substrate-precipitate, precipitate-solution, and substrate-solution. When the ratio of the substrate surface area to solution volume is high, the substrate-precipitate interfacial energy may drive ACC formation and potentially phase selection. It could be that the ACC-CPG interfacial energy is sufficiently low, relative to the interfacial energies of the crystalline phases to CPG, that it overcomes the more favorable bulk free energy of the crystalline phases. Anion exclusion may be an alternative explanation. That is, the negative surface charges expected within the nanopores at pH 8.4 create a local nanopore environment where calcium-to-carbonate ratios are much higher than in the original solution.[3] Very high calcium-to-carbonate ratios have produced flocs of material out of solution at similar pH values.[36,56] It is possible that contradictory theories for the pore-size dependence of precipitation could be resolved accounting for these substrate-precipitate interactions, and the surface area to fluid volume ratio of the porous medium.

Conclusions

We have observed a monohydrocalcitic-ACC precipitate forming within a nanoporous CPG substrate under solution conditions thermodynamically favoring calcite, aragonite, or vaterite formation, but not ACC or monohydrocalcite. The observation that the presence of nanopores (high ratio of substrate surface area to solution volume) can affect carbonate phase growth and possible phase selection has obvious implications for precipitation in the subsurface, suggesting that the solubility product alone, or kinetic measurements of nucleation/growth in open solution, are not sufficient to predict which phase(s) will form in confined environments. Our results demonstrate another key factor in determining structural formation and stability of ACC phases/precursors. We summarize in Figure 4, a schematic diagram, on the various reported chemical and physical controls identified in the literature for ACC formation and stability.

We have also demonstrated the sensitivity of difference PDF for tracking the identity, rate, and size of very small precipitates forming out of flowing carbonate solution in CPG: a reasonable proxy for studying precipitation in rock. The methods can readily be modified to investigate the influence of flow rate, temperature, pore size, saturation levels, pore-wall chemistry, additives, etc. on the precipitation, growth and

stabilization of metastable phases. It would be fascinating to try the same with neutron PDF, where the behavior and influence of (heavy) water on these processes may be observed.

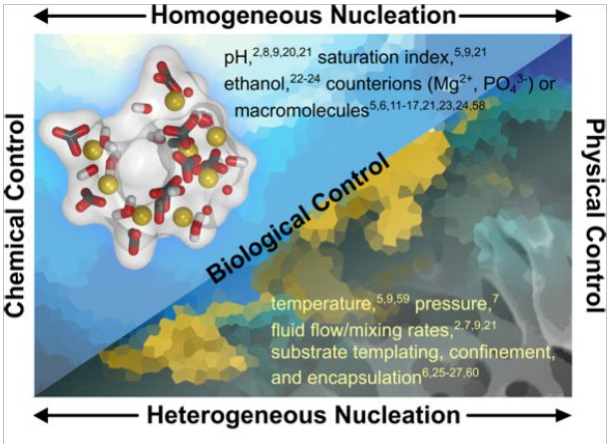

Figure 4. Chemical and physical factors reported to impact or improve the formation or stabilization of amorphous calcium carbonates (representative references are noted). Both chemical and physical factors are harnessed in the biological control of phases.

Conflicts of interest

There are no conflicts to declare.

Acknowledgements

The work by all authors was supported under the Department of Energy's Office of Basic Energy Sciences. K.P. was supported through the U.S. Department of Energy, Office of Science, Office of Basic Energy Sciences, Early Career Research Program Award KC040602. H.-W.W., A.G.S. and S.A.C. were supported through the U.S. Department of Energy, Office of Science, Office of Basic Energy Sciences, Chemical Sciences, Geosciences, and Biosciences Division. Research at the 11-ID-B beamline used resources of the Advanced Photon Source, a U.S. Department of Energy, Office of Science. User Facility operated for the Department of Energy's Office of Science by Argonne National Laboratory under Contract No. DE-AC02-06CH11357. The authors thank Kevin Bayer for technical support at the 11-ID-B beamline. The monohydrocalcite sample (NMNH 135404 00) is provided from the mineral collection of the Department of Mineral Sciences, Smithsonian Institution.

References

1 P. Raiteri and J. D. Gale, Water Is the Key to Nonclassical Nucleation of Amorphous Calcium Carbonate, *J. Am. Chem. Soc.*, 2010, **132**, 17623-17634.
2 D. Gebauer, A. Volkel and H. Colfen, Stable Prenucleation Calcium Carbonate Clusters, *Science*, 2008, **322**, 1819-1822.
3 A. G. Stack, Precipitation in Pores: A Geochemical Frontier, *Rev. Mineral. Geochem.*, 2015, **80**, 165-190.
4 H.-W. Wang, K. Yuan, N. Rampal and A. G. Stack, Solution and Interface Structure and Dynamics in Geochemistry: Gateway to Link Elementary Processes to Mineral Nucleation and Growth, *Cryst. Growth Des.*, 2022, **22**, 853–870.
5 J. H. Cartwright, A. G. Checa, J. D. Gale, D. Gebauer and G. I. Sainz-Diaz, Calcium Carbonate Polyamorphism and its Role in Biomineralization: How Many Amorphous Calcium Carbonates are There? *Angew. Chem. Int. Ed. Engl.*, 2012, **51**, 11960-11970.
6 S. Weiner, Y. Levi-Kalisman, S. Raz and L. Addadi, Biologically Formed Amorphous Calcium Carbonate, *Connect Tissue Res.*, 2003, **44**, 214-218.
7 A. Fernandez-Martinez, B. Kalkan, S. M. Clark and G. A. Waychunas, Pressure-induced Polyamorphism and Formation of 'Aragonitic' Amorphous Calcium Carbonate, *Angew. Chem. Int. Ed.*, 2013, **52**, 8354-8357.
8 D. Gebauer, P. N. Gunawidjaja, J. Y. Ko, Z. Bacsik, B. Aziz, L. Liu, Y. Hu, L. Bergstrom, C. W. Tai, T. K. Sham, M. Eden and N. Hedin, Proto-calcite and Proto-vaterite in Amorphous Calcium Carbonates, *Angew. Chem. Int. Ed. Engl.*, 2010, **49**, 8889-8891.
9 H.-W. Wang, L. L. Daemen, M. C. Cheshire, M. K. Kidder, A. G. Stack, L. F. Allard, J. C. Neuefeind, D. Olds, J. Liu and K. Page, Synthesis and Structure of Synthetically Pure and Deuterated Amorphous (Basic) Calcium Carbonates, *Chem. Commun.*, 2017, **53**, 2942-2945.
10 M. F. Khouzani, D. M. Chevrier, P. Güttlein, K. Hauser, P. Zhang, N. Hedin and D. Gebauer, Disordered Amorphous Calcium Carbonate from Direct Precipitation, *CrystEngComm*, 2015, **17**, 4842-4849.
11 S. K. Raymond, J. M. Lam, A. L. Charnock and F. C. Meldrum, Synthesis-Dependent Structural Variations in Amorphous Calcium Carbonate, *CrystEngComm,* 2007, **9**, 1226-1236.
12 B. Guillemet, M. Faatz, F. Gröhn, G. Wegner and Y. Gnanou, Nanosized Amorphous Calcium Carbonate Stabilized by Poly(ethylene oxide)-b-poly (acrylic acid) Block Copolymers, *Langmuir* 2006, **22**, 1875-1879.
13 A. Gal, S. Weiner and L. Addadi, The Stabilizing Effect of Silicate on Biogenic and Synthetic Amorphous Calcium Carbonate, *J. Am. Chem. Soc.*, 2010, **132**, 13208-13211.
14 M. Kellermeier, E. Melero-Garcia, F. Glaab, R. Klein, M. Drechsler, R. Rachel, J. M. García-Ruiz and W. Kunz, Stabilization of Amorphous Calcium Carbonate in Inorganic Silica-Rich Environments, *J. Am. Chem. Soc.*, 2010, **132**, 17859-17866.
15 S. Kababya, A. Gal, K. Kahil, S. Weiner, L. Addadi and A. Schmidt, Phosphate–Water Interplay Tunes Amorphous Calcium Carbonate Metastability: Spontaneous Phase Separation and Crystallization vs Stabilization Viewed by Solid State NMR, *J. Am. Chem. Soc.*, 2015, **137**, 990-998.
16 M. Alberic, L. Bertinetti, Z. Zou, P. Fratzl, W. Habraken and Y. Politi, The Crystallization of Amorphous Calcium Carbonate is Kinetically Governed by Ion Impurities and Water, *Adv. Sci.*, 2018, **5**, 1701000.
17 A. AKoishi, A. Fernandez-Martinez, B. Ruta, M. Jimenez-Ruiz, R. Poloni, D. di Tommaso, F. Zontone, G. A. Waychunas and G. Montes-Hernandez, Role of Impurities in the Kinetic Persistence of Amorphous Calcium Carbonate: A Nanoscopic Dynamics View, *J. Phys. Chem. C*, 2018, **122**, 16983-16991.
18 S. Leukel, M. Panthöfer, M. Mondeshki, G. Kieslich, Y. Wu, N. Krautwurst and W. Tremel, Trapping Amorphous Intermediates of Carbonates – A Combined Total Scattering and NMR Study, *J. Am. Chem. Soc.*, 2018, **140**, 14638–14646
19 D. Gebauer and S. E. Wolf, Designing Solid Materials from Their Solute State: A Shift in Paradigms toward a Holistic Approach in Functional Materials Chemistry, *J. Am. Chem. Soc.*, 2019, **141**, 4490-4504.
20 D. J. Tobler, J. D. Rodriguez-Blanco, H, O. Sørensen, S. L. S. Stipp and K. Dideriksen, Effect of pH on Amorphous Calcium Carbonate Structure and Transformation, *Cryst. Growth Des.*, 2016, **16**, 4500-4508.
21 C. R. Blue, A. Giuffrea, S. Mergelsberga, N. Hana, J. J. De Yoreo and P. M. Dovea, Chemical and Physical Controls on the Transformation of Amorphous Calcium Carbonate into

Crystalline $CaCO_3$ polymorphs, *Geochim. Cosmochim. Acta*, 2017, **196**, 179-196.
22 S. F. Chen, H. Colfen, M. Antonietti and S. Yu, Ethanol Assisted Synthesis of Pure and Stable Amorphous Calcium Carbonate Nanoparticles, *Chem. Commun.*, 2013, **49**, 9564-9566.
23 Z. Lei, S. Sun and P. Wu, Ultrafast, Scale-Up Synthesis of Pure and Stable Amorphous Carbonate Mineral Nanoparticles, *ACS Sustain. Chem. Eng.*, 2017, **5**, 4499-4504.
24 R. Sun, P. Zhang, E. G. Bajnoczi, A. Neagu, C. W. Tai, I. Persson, M. Stromme and O. Cheung, Amorphous Calcium Carbonate Constructed from Nanoparticle Aggregates with Unprecedented Surface Area and Mesoporosity, *ACS Appl. Mater. Interfaces*, 2018, **10**, 21556-21564.
25 C. C. Tester, R. E. Brock, C.-H. Wu, M. R. Krejci, S. Weigand and D. Joester, In vitro Synthesis and Stabilization of Amorphous Calcium Carbonate (ACC) Nanoparticles within Liposomes, *Cryst. Eng. Comm.*, 2011, **13**, 3975 – 3978.
26 C. J. Stephens, S. F. Ladden, F. C. Meldrum and H. K. Christenson, Amorphous Calcium Carbonate is Stabilized in Confinement, *Adv. Funct. Mater.*, 2010, **20**, 2108-2115.
27 J. Ihli, C. W. Wong, E. H. Noel, Y. Y. Kim, A. N. Kulak, H. K. Christenson, M. J. Duer and F. C. Meldrum, Dehydration and Crystallization of Amorphous Calcium Carbonate in Solution and in Air, *Nat. Commun.*, 2014, **5**, 3169.
28 A. G. Stack, A. Fernandez-Martinez, L. F. Allard, J. L. Banuelos, G. Rother, L. M. Anovitz, D. R. Cole and G. A. Waychunas, Pore-size-dependent Calcium Carbonate Precipitation Controlled by Surface Chemistry, *Environ. Sci. Technol.*, 2014, **48**, 6177-6183.
29 P. J. Chupas, K. W. Chapman, G. Jennings, P. L. Lee and C. P. Grey, Watching Nanoparticles Grow: The Mechanism and Kinetics for the Formation of TiO_2-Supported Platinum Nanoparticle, *J. Am. Chem. Soc.*, 2007, **129**, 13822**–**13824.
30 K. M. Ø. Jensen, M. Christenson, P. Juhas, C. Tyrsted, E. D. Bøjeson, N. Lock, S. J. L. Billinge and B. B. Iverson, Revealing the Mechanisms behind SnO_2 Nanoparticle Formation and Growth During Hydrothermal Synthesis: An in situ Total Scattering Study, *J. Am. Chem. Soc.*, 2012, **134**, 6785-6792.
31 H. Kim, A. Karkamkar, T. Autrey, P. J. Chupas and T. Proffen, Determination of Structure and Phase Transition of Light Element Nanocomposites in Mesoporous Silica: Case study of NH_3BH_3 in MCM-41, *J. Am. Chem. Soc.*, 2003, **131**, 13749-13755.
32 H.-W. Wang, D. J. Wesolowski, T. Proffen, L. Vlcek, W. Wang, L. F. Allard, A. I. Kolesnikov, M. Feygenson, L. M. Anovitz and R. L. Paul, Structure and Stability of SnO_2 Nanocrystals and Surface-Bound Water Species, J*. Am. Chem. Soc.*, 2013, **135**, 6885-6895.
33 M. L. Beauvais, P. J. Chupas, D.l O'Nolan, J. B. Parise and K. W. Chapman, Resolving Single-layer Nanosheets as Short-lived Intermediates in the Solution Synthesis of FeS, ACS Materials Lett., 2021, **3**, 698**–**703.
34 P. J. Chupas, X. Qiu, J. C. Hanson, P. L. Lee, C. P. Grey and S. J. L. Billinge, Rapid-acquisition Pair Distribution Function (RA-PDF) Analysis, *J. Appl. Crystallogr.*, 2003, **36**, 1342-1347.
35 D. L. Parkhurst, User's Guide to PHREEQE—a Computer Program for Speciation, Reaction-path, Advective Transport, and Inverse Geochemical Calculations, *US Geological Survey Water-Resources Investigations Report*, 1995.
36 A. G. Stack, Next generation models of carbonate mineral growth and dissolution. *Greenhouse Gas. Sci. Technol.,* 2014, **4**, 278.
37 J. W. Morse and F. T. Mackenzie, *Geochemistry of Sedimentary Carbonates*, 1990, 48, Elsevier.
38 L. N. Plummer and E. Busenberg, The Solubilities of Calcite, Aragonite and Vaterite in CO_2-H_2O Solutions between 0 and 90°C, and an Evaluation of the Aqueous Model for the system $CaCO_3$-CO_2-H_2O, *Geochim. Cosmochim. Acta*, 1982, **46**, 1011-1040.
39 L. Brečević and D. Kralj, On Calcium Carbonates: from Fundamental Research to Application, *Croat. Chem. Acta*, 2007, **80**, 467-484.
40 J. L. Bischoff, J. A. Fitzpatrick and R. J. Rosenbauer, The Solubility and Stabilization of Ikaite ($CaCO_{3.6}H_2O$) from 0˚ to 25˚C: Environmental and Paleoclimatic Implications for Thinolite Tufa. *J. Geol.*, 1993, 21-33.
41 L. Brečević, A. E. Nielsen, Solubility of Amorphous Calcium Carbonate, *J. Cryst. Growth*, 1989, **98**, 504-510.
42 T. Ogino, T. Suzuki and K. Sawada, The Formation and Transformation Nechanism of Calcium Carbonate in Water, *Geochim. Cosmochim. Acta*, 1987, **51**, 2757-2767.
43 F. M. Michel, J. MacDonald, J. Feng, B. L. Phillips, L. Ehm, C. Tarabrella, J. B. Parise and R. J. Reeder, Structural Characteristics of Synthetic Amorphous Calcium Carbonate, *Chem. Mater.*, 2008, **20**, 4720-4728.
44 A. L. Goodwin, F. M. Michel, B. L. Phillips, D. A. Keen, M. Dove, R. J. Reeder, Nanoporous Structure and Medium-Range Order in Synthetic Amorphous Calcium Carbonate *Chem. Mater.*, 2010, **22**, 3197-3205.
45 M. P. Prange, S. T. Mergelsberg and S. N. Kerisit, Ab Initio Molecular Dynamics Simulations of Amorphous Calcium Carbonate: Interpretation of Pair Distribution Function and X-ray Absorption Spectroscopy Data, *Cryst. Growth Des.*, 2021, **21**, 2212-2221.
46 H. Hull and A. G. Turnbull, A Thermochemical Study of Monohydrocalcite, *Geochim. Cosmochim. Acta*, 1973, **37**, 685**–**694.
47 H. Marschner, Hydrocalcite ($CaCO_3$-H_2O) and Nesquehonite ($MgCO_3$-$3H_2O$) in Carbonate Scales, *Science*, 1969, **165**, 1119-1121.
48 K. Dahl and B. J. Buchardt, Monohydrocalcite in the Arctic Ikka Fjord, SW Greenland: First Reported Marine Occurrence, *Sediment. Res.*, 2006, **76**, 460-471.
49 H. Catherine, K. Skinner, G. W. Osbaldiston and A. N. Wilner, Monohydrocalcite in a Guinea Pig Bladder Stone, a Novel Occurrence, *Am. Mineral.*, 1977, **62**, 273-277.
50 M. Señorale-Pose, C. Chalara, Y. Dauphin, P. Massard, P. Pradel and M. Marína, Monohydrocalcite in Calcareous Corpuscles of Mesocestoides Corti, *Exp. Parasitol.*, 2007, **118**, 54-58.
51 L. A. J. Garvie, Decay-induced Biomineralization of the Saguaro Cactus (Carnegiea Gigantea), *Am. Mineral.*, 2003, **88**, 1879-1888.
52 Y.-Y. Wang, Q.-Z. Yao, G.-T. Zhou and S.-Q. Fu, Transformation of Amorphous Calcium Carbonate into Monohydrocalcite in Aqueous Solution: A Biomimetic Mineralization Study. *Eur. J. Mineral.*, 2015, **27**, 717-729.
53 J. D. Rodriguez-Blanco, S. Shaw, P. Bots, T. Roncal-Herrero and L. G. Benning, The Role of Mg in the Crystallization of Monohydrocalcite, *Geochim. Cosmochim. Acta*, 2014, **127**, 204-220.
54 N. Deng, A. G. Stack, J. Weber, B. Cao, J. J. De Yoreo and Y. Hu, Organic-Mineral Interfacial Chemistry Drives Heterogeneous Nucleation of Sr-rich (Ba_x,Sr_{1-x})SO_4 from Undersaturated Solution, *PNAS*, 2019, **116**, 13221-13226.
55 J. J. De Yoreo and P. G. Vekilov, Principles of Crystal Nucleation and Growth, *Rev. Mineral. Geochem.*, 2003, **54**, 57-94.
56 T. A. Gebrehiwet, G. D. Redden, Y. Fujita, M. S. Beig and R. W. Smith, The Effect of the CO_3^{2-} to Ca^{2+} Ion Activity Ratio on Calcite Precipitation Kinetics and Sr^{2+} Partitioning, *Geochem. Trans.*, 2012, **13**, 1-11.
57 C. L. Farrow, P. Juhás, J. W. Liu, D. Bryndin, E. S. Božin, J. Bloch, T. Proffen and S. J. L. Billinge, PDFfit2 and PDFgui:

computer programs for studying nanostructure in crystals, *J. Phys.: Condens. Mat*., 2007, **19**, 335219.
58 L. B. Gower, Biomimetic Model Systems for Investigating the Amorphous Precursor Pathway and its Role in Biomineralization, *Chem. Rev.*, 2008, **108**, 4551-4627.
59 J. Ihli, A. N. Kulak and F. C. Meldrum, Freeze-drying Yields Stable and Pure Amorphous Calcium Carbonate (ACC), *Chem. Commun.*, 2013, **49**, 3134-3136.
60 E. M. Pouget, P. H. Bomans, J. A. Goos, P. M. Frederik, G. de With and N. A. Sommerdijk, The Initial Stages of Template-Controlled $CaCO_3$ Formation Revealed by Cryo-TEM, *Science*, 2009, **323**, 1455-1458.